Dating the Vostok ice core by an inverse method

Frédéric Parrenin, Jean Jouzel, Claire Waelbroeck, Catherine Ritz, Jean-Marc Barnola

JOURNAL OF GEOPHYSICAL RESEARCH, VOL. 106, NO. D23, PAGES 31,837–31,851, DECEMBER 16, 2001

Dating the Vostok ice core by an inverse method

Frédéric Parrenin,[1,2] Jean Jouzel,[1] Claire Waelbroeck,[1] Catherine Ritz,[2] and Jean-Marc Barnola[2]

Abstract. Using the chronological information available in the Vostok records, we apply an inverse method to assess the quality of the Vostok glaciological timescale. The inversion procedure provides not only an optimized glaciological timescale and its confidence interval but also a reliable estimate of the duration of successive events. Our results highlight a disagreement between orbitally tuned and glaciological timescales below ~2700 m (i.e., ~250 kyr B.P., thousands of years before present). This disagreement could be caused by some discontinuity in the spatial variation of accumulation upstream of Vostok. Moreover, the stratigraphic datings of central Greenland ice cores (GRIP and GISP2) appear older than our optimized timescale for the late glacial. This underlines an unconsistency between the physical assumptions used to construct the Vostok glaciological timescale and the stratigraphic datings. The inverse method allows the first assessment of the evolution of the phase between Vostok climatic records and insolation. This phase significantly varies with time which gives a measure of the nonlinear character of the climatic system and suggests that the climatic response to orbital forcing is of different nature for glacial and interglacial periods. We confirm that the last interglacial, as recorded in the Vostok deuterium record, was long (16.2 ± 2 kyr, thousands of years). However, midtransition of termination II occurred at 133.4 ± 2.5 kyr BP, which does not support the recent claim for an earlier deglaciation. Finally, our study suggests that temperature changes are correctly estimated when using the spatial present-day deuterium-temperature relationship to interpret the Vostok deuterium record.

1. Introduction

Exploiting the wealth of climatic information contained in deep ice cores from Greenland and Antarctica requires accurate dating of the various temporal series obtained either from the ice matrix or from the air bubbles trapped in the ice. For example, the deuterium (δD) and/or oxygen 18 ($\delta^{18}O$) concentration of the Vostok ice (central East Antarctica) give access to parameters such as the temperature of the site [*Jouzel et al.*, 1993, 1987] and the origin of the precipitation [*Vimeux et al.*, 1999]. This ice also contains information on changes in the atmospheric circulation and in the hydrological cycle through aerosol fallout [*de Angelis et al.*, 1985; *Petit et al.*, 1990]. Elemental composition of the air bubbles gives access to changes in greenhouse gases [*Barnola et al.*, 1987; *Chappellaz et al.*, 1990] and in other gaseous compounds. Their isotopic composition also contains climate-related information such as that derived from the isotopic composition of the oxygen in air (hereinafter $\delta^{18}O_{atm}$) which is related to the hydrological cycle in the tropics and to sea level change [*Bender et al.*, 1994a; *Jouzel et al.*, 1996; *Sowers et al.*, 1993]. All the Vostok records (δD, $\delta^{18}O$, and aerosol concentration in the Vostok ice, greenhouse gases, CO_2 and CH_4, and $\delta^{18}O_{atm}$ in the air bubbles) are now available down to a depth slightly deeper than 3300 m and cover the last four glacial–interglacial cycles [*Petit et al.*, 1999; *Vimeux et al.*, this issue].

Various methods are used to date ice cores. They fall into four categories: (1) layer counting, (2) glaciological modeling, (3) use of time markers and correlation with other dated time series, and (4) comparison with insolation changes (i.e., orbital tuning). Layer counting is not feasible in low accumulation areas such as central Antarctica where the Vostok site is located. For the Vostok core, a modeling approach combining an ice flow model [*Ritz*, 1992] and an accumulation model has been developed for dating the first climatic cycle [*Lorius et al.*, 1985]. It was further extended to two [*Jouzel et al.*, 1993, 1996] and recently to four climatic cycles [*Petit et al.*, 1999] back to 420 kyr BP. Vostok chronologies have also been derived by correlation with marine records dated by orbital tuning (SPECMAP chronology, *Martinson et al.* [1987]), using either dust content [*Petit et al.*, 1990], temperature changes [*Pichon et al.*, 1992; *Shackleton et al.*, 1992], $\delta^{18}O_{atm}$ [*Sowers et al.*, 1993], or CO_2 concentration [*Raymo and Horowitz*, 1996]. An orbital tuning approach similar to that developed to define the SPECMAP chronology has also been applied [*Raymo and Horowitz*, 1996; *Salamatin et al.*, 1998a; *Waelbroeck et al.*, 1995; *Shackleton*, 2000]. Finally, the age of the gas is younger than the age of the ice due to the fact that air bubbles are trapped when firn closes off at depth. The ice age–gas age difference, Δage, is currently estimated as a function of temperature and accumulation through a firnification model [*Barnola et al.*, 1991; *Schwander et al.*, 1997].

Each of these approaches has advantages and drawbacks. Orbitally tuned chronologies have associated uncertainties relatively constant along the entire record, which should not exceed a few thousands of years. However, they do not allow to infer climatic information from the phasing between Vostok series and insolation curves or other climate records. This also

[1] Laboratoire des Sciences du Climat et de l'Environnement, Gif-Sur-Yvette, France.

[2] Laboratoire de Glaciologie et Géophysique de l'Environnement, Grenoble, France.

Paper number 2001JD900245.
0148-0227/01/2001JD900245$09.00

holds true for correlated chronologies. Moreover, both orbitally tuned and correlated chronologies may imply locally unrealistic accumulation rates, and this prevents a correct estimate of the duration of successive climatic events. Instead, glaciological timescales are consistent with respect to both ice flow laws and accumulation processes, but the dating error then increases with depth, and in order to keep this error in reasonable bounds, control points (i.e., depths with assigned ages) are needed along the profile. These control points are themselves derived from correlation with other records or with insolation changes, so a glaciological timescale is not truly independent of some assumptions on the phasing between Vostok records and other time series. Also, the glaciological timescale is based on assumptions that are subject to discussion such as the use of the present-day spatial deuterium–temperature relationship to interpret the Vostok deuterium record and infer accumulation change. Moreover, it relies on poorly defined values of the melting and the sliding rates at the bottom of the ice sheet. As a result the uncertainty of the current Vostok glaciological timescale (GT4, *Petit et al.*, [1999]) may be as high as ± 15 kyr.

Here we try to combine the advantages of the glaciological approach and of the orbital tuning in order to minimize the limitations mentioned above. To this end, we no longer make any assumption about the phase relationship between insolation and Vostok records but simply assume that we can correctly count the number of precessional cycles in those records. This appears straightforward considering how this cycle is clearly imprinted in the $\delta^{18}O_{atm}$ series [*Jouzel et al.*, 1996; *Petit et al.*, 1999]. To express this assumption, we simply assign the ice and gas chronologies to pass through a succession of large doors (see below). In addition, we take advantage of the fact that the Vostok core is accurately dated back to ~7 kyr BP by matching cosmogenic production rates of beryllium 10 measured in this core with that of carbon 14 measured in dated trees [*Raisbeck et al.*, 1998], to derive time constraints over this recent period. We also take advantage of the beryllium 10 peak which is present in the Vostok ice core and that has been dated by several studies (for a recent review, see *Schramm et al.* [2000]). We use a Monte Carlo inverse method based on the Metropolis Hastings algorithm to determine the accumulation and ice flow parameters in order to obtain a range of glaciological timescales (both for the ice and the gas) in good agreement with this given chronological information.

We first describe the ice flow and accumulation models used to derive the current glaciological timescale and examine the aspects on which it can be improved. One of the most important modifications we propose deals with the use of prior chronological information. This is discussed in the following section, which focuses on how we account for orbital constraints. We then present the inversion procedure and discuss the results of the experiments we have performed. We show that if we adopt a simple formulation of spatial accumulation change, the glaciological approach is unable to provide a timescale matching orbital constraints beyond the last two climatic cycles or so. Beyond providing an improved glaciological timescale over this period, and its interval of confidence, the inverse method brings estimates of the accumulation around Vostok and of past temperature changes. We then compare our results with other ice core chronologies and examine the phasing between Vostok series and insolation.

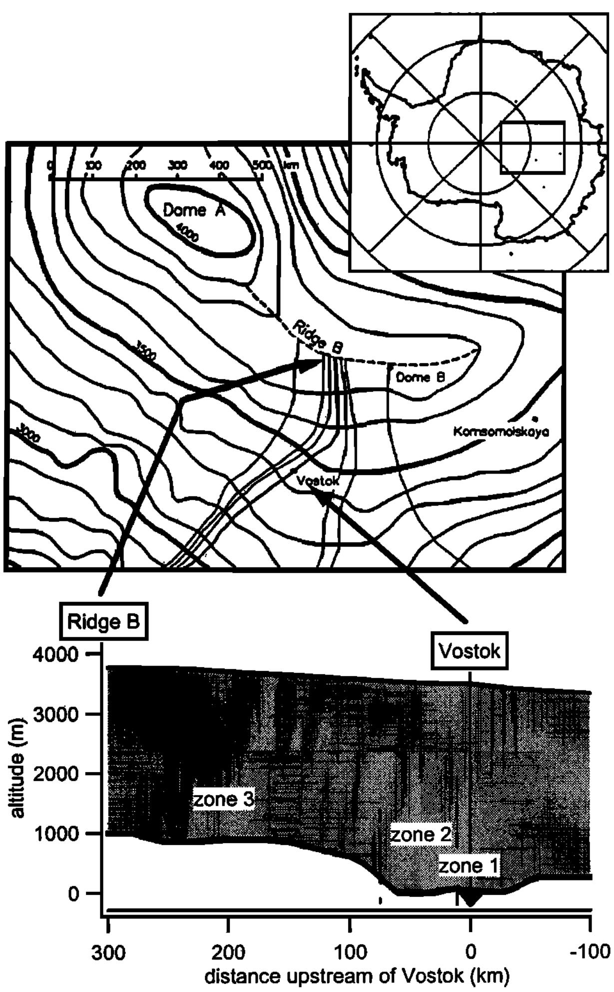

Figure 1. Vostok – Ridge B ice flow line. Zone 1, Vostok Lake area (freezing and sliding). Zone 2, temperate base (melting). Zone 3, cold base (no melting and no sliding).

2. Glaciological Timescale

2.1. Current GT4 Timescale

To compute the age of an ice layer, we need to estimate the rate of accumulation at that time and the thinning function, i.e. the ratio of the thickness of a layer to its initial thickness. The age of the ice at a given depth z is then calculated through:

$$\mathrm{age}(z)=\int_0^z \frac{dy}{\mathrm{accumulation}(y)\times\mathrm{thinning}(y)}.$$

The current GT4 (Glaciological Timescale four cycles) timescale [*Petit et al.*, 1999] is established using this approach. The thinning function is computed by the 2½ dimensional flow model developed by [*Ritz*, 1992] accounting for the fact that the Vostok ice originates from the area between Ridge B, upstream of Vostok, and the Vostok site (Figure 1). The third dimension is taken into account with the convergence of ice flow lines. The variations of surface elevation between Vostok and Ridge B are computed by integrating the accumulation rate minus its mean value. The velocity of the ice is calculated in two steps. First, the mean horizontal velocity is derived from the mass balance equation (taking into account the accumulation at the top of the ice sheet and the melting at the base). Second, the vertical velocity profile is calculated accounting for the sliding rate at the base of the ice sheet (the ratio of the velocity of ice near the bedrock to the velocity balance) and for the deformation profile computed analytically using the ice flow equations. Ice velocity equations are then integrated backward in time along ice flow lines allowing to calculate the thinning as a function of depth.

The accumulation rate is estimated from the temperature at the level where precipitation forms (which is close to the inversion temperature T_i) , and from the distance x, from Vostok [*Jouzel et al.*, 1993]:

$$\text{Accumulation}=\text{Acc}^\circ(x)\times f(T_i)/f(T_i^\circ),$$

where Acc° is the accumulation at a reference temperature T_i°. The GT4 timescale is based on the following assumptions: First, the accumulation rate varied in the past as a function of the derivative of the water vapor saturation pressure with respect to the inversion temperature:

$$f(T_i)=\frac{d}{dT}\left(\frac{Ps(T)}{T}\right)\Bigg|_{T=T_i}.$$

Second, the accumulation upstream of Vostok, where ice found at depth originates, linearly increases as a function of the distance from Vostok (i.e., Acc° is linear), and accumulation at Ridge B is deduced from the Dome B deep ice core. Third, after applying a correction for the change in the seawater isotopic content, past temperatures are estimated using the present-day spatial relationship between deuterium content and surface temperature. Fourth, the depths corresponding to the ages of 110 and 390 kyr BP are assigned (control points). There are only three adjustable parameters in this version of the model: the rate of present-day accumulation at Vostok and the melting and sliding rates around Vostok.

The GT4 timescale has then been established by direct modeling until an appropriate set of the adjustable parameters matched the two control points [*Petit et al.*, 1999]. This gives the age of the ice over the last four climatic cycles (420 kyr BP) with an accuracy estimated to be always better than ± 15 kyr. The age of the gas is calculated applying the firnification model of *Barnola et al.* [1991]. In the present study we will use the GT4 ice and gas timescales as reference timescales.

2.2. Toward an Improved Glaciological Timescale

Although useful for interpreting Vostok climatic time series and well adapted for comparing the various records that can be extracted from the Vostok ice and from the entrapped air bubbles, the assumptions that served to establish the GT4 timescale are subject to debate. First, the present day deuterium-temperature relationship clearly underestimates (by up to a factor of 2) past temperature changes for Greenland (*Jouzel* [1999], and references herein for a recent review). There are reasons why differences should not be so large for Antarctica [*Caillon et al.*, this issue; *Delaygue et al.*, 2000; *Hoffmann et al.*, 2000; *Petit et al.*, 1999], but still, the use of the present-day relationship may not be optimal. Second, assuming that past accumulation varied only as a function of the vapor pressure may be too simplistic. Third, the assumption of a linear accumulation increase between Vostok and Ridge B is not guaranteed as we have access to present-day accumulation in two sites only, Vostok and Dome B [*Jouzel et al.*, 1995]. Moreover, this latter drilling site is located on Ridge B but relatively far, i.e., more than 100 km, from the area where the Vostok ice comes from. Fourth, the influence of the Vostok Lake on the parameters of the ice flow model should be better taken into account than previously. Fifth, a better use of the various chronological information available is certainly possible and no uncertainty is associated with the definition of the time control points whereas it should be the case. To account, as much as possible, for these various potential sources of uncertainty, we propose the following improvements:

First, rather than assuming a linear relationship between the ice deuterium content and surface temperature and imposing its slope, we simply use a second-order relationship with two free parameters, α and β. We express the temperature change at the inversion level as $\Delta T_i = \alpha \bullet \Delta(\delta D) + \beta \bullet \Delta(\delta D)^2$. In doing so, we make no assumption on the size of the glacial-interglacial temperature change. On the contrary, the use of available chronological information places interesting constraints on temperature change (see results).

Second, the existence of a linear relationship between the accumulation and the derivative of the saturation pressure is based on a one-dimensional atmospheric transport model which is probably justified over central East Antarctica where meteorological conditions are simple. However, other parameters than temperature such as the intensity of the atmospheric circulation may influence accumulation rates. Here we have kept the formulation adopted to establish GT4, because we have not enough information to independently constrain the accumulation rate and the temperature. However, we discuss the possible influence of atmospheric circulation changes.

As far as the spatial change of accumulation is concerned, we adopt the same approach as for temperature estimate, i.e., we assume that this accumulation is a second-order function of the distance to Vostok and do not impose the parameter values: $Acc^\circ(x) = a + bx + cx^2$. In addition, the position in depth of the last glacial-interglacial transition in the Dome B ice core provides a constraint on the accumulation at Dome B, which we extend to Ridge B (100 km far from Dome B): Acc°(Ridge B)=3±0.5 cm of ice/year. The 0.5 uncertainty accounts for the uncertainty on Dome B accumulation rate, and for the fact that this latter site is located about 100 km from the area of origin of the Vostok ice.

Concerning the ice flow model, uncertainties on the thinning value mainly come from the poor knowledge of the sliding and of the melting at the base of the ice sheet. As illustrated in Figure 1, three different areas can be distinguished in the region between the Ridge B axis and the Vostok Lake with respect to basal conditions: (1) the Vostok Lake area [*Kapitza et al.*, 1996] which extends ~15 km in the direction of Ridge B (zone 1), (2) the region between 15 and 75 km from Vostok (zone 2), where the base is expected to reach the melting point [*Petit et al.*, 1999; *Ritz*, 1992] because of an important ice sheet thickness (temperate base), and (3) the region near Ridge B (zone 3) where because of a smaller ice sheet thickness, there is probably no melting and no sliding (cold base). The GT4 timescale makes no distinction between the first two regions and assumes a sliding rate of 70% and a melting rate of 0.4 mm/year. Instead, we distinguish between these two zones and account for the freezing that takes place from the Lake Vostok water below the ice sheet [*Jouzel et al.*, 1999]. We have fixed the sliding to reasonable values in zone 1 (90 %) and assume no sliding for zone 2, whereas we let open the melting rate values for those two regions (denoted, respectively, by m_1 and m_2). We, however, account for the fact that a simple energy balance indicates that the freezing rate at the surface of the Vostok Lake do not exceed 4 mm/year [*Salamatin et al.*, 1998b].

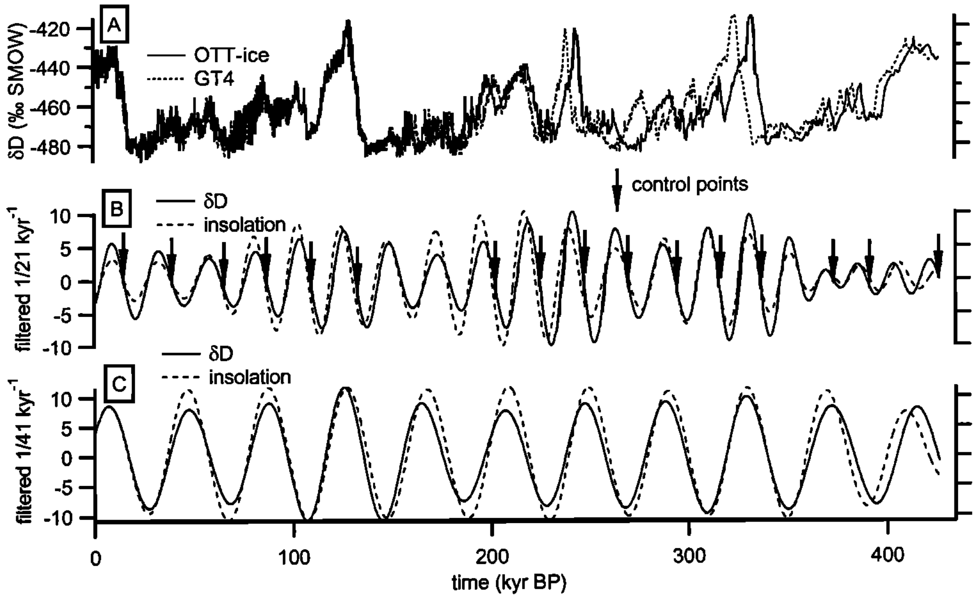

Figure 2. Vostok δD record (A) and its 1/20 kyr^{-1} (B) and 1/40 kyr^{-1} (C) components in the orbitally tuned chronology (solid lines), compared to those of insolation, shifted by –3000 years (dashed lines); δD is also presented in the GT4-ice chronology for reference (dotted line). Vertical arrows show where control points have been placed to construct the OTTice timescale from GT4-ice (the last control point, just used to constrain approximately the end of the signal, is uncertain).

Concerning the Δage calculation (ice age–gas age difference at a given depth), we have used the semiempirical firn model of Pimienta and Barnola [*Barnola et al.*, 1991], constrained with the accumulation and temperature described above.

The most important modification in our approach with respect to GT4 is the use of available a priori chronological information. We have to constrain the poorly known parameters described above. Rather than having fixed control points as in GT4, the principle is here to account for the uncertainty associated with any chronological information, by applying an inverse method which identifies glaciological chronologies that best fit this information (see below). The way we use this chronological information is described in section 3.

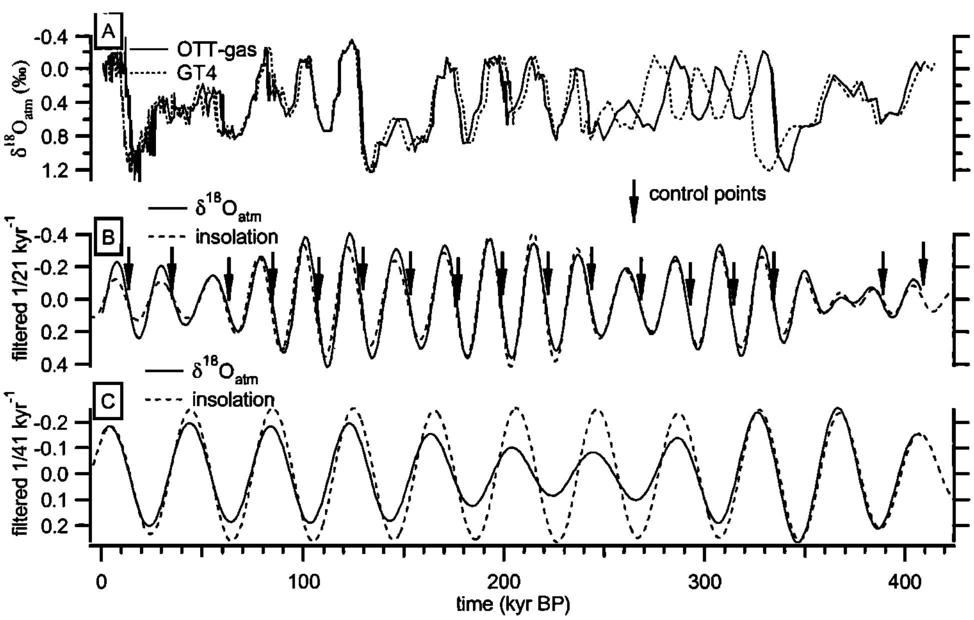

Figure 3. Vostok $\delta^{18}O_{atm}$ record (A) and its 1/20 kyr^{-1} (B) and 1/40 kyr^{-1} (C) components in the orbitally tuned chronology (solid lines), compared to those of insolation, shifted by -5500yr (dashed lines); $\delta^{18}O_{atm}$ is also presented in the GT4-gas chronology for reference (dotted line). Vertical arrows show where control points have been placed to construct the OTT-gas timescale from GT4-gas (the last control point, just used to constrain approximately the end of the signal, is uncertain).

3. Chronological Information

The primary source of chronological information that we will use comes from the fact that orbital frequencies are clearly imprinted in most Vostok series [*Petit et al.*, 1999], in particular in the ice deuterium (temperature proxy) and $\delta^{18}O_{atm}$ records. Our approach simply assumes that we can correctly count the number of precessional cycles (frequencies at 19 and 23 kyr) in those records. This broadly corresponds to the idea that the phase between the insolation and the Vostok series never exceeds half a precessional cycle [*Jouzel et al.*, 1996]. To express this idea, we use control doors, i.e., control points with associated uncertainties. As discussed below, we use either Gaussian doors with a width of ± 6 kyr at midheight or rectangular doors with a total width of 12 kyr. To define the center of these doors, we first derive independent orbitally tuned Vostok timescales for the ice (from the deuterium record) and for the gas (from the $\delta^{18}O_{atm}$ record), respectively.

As far as the deuterium is concerned, we have simply extended to the full record the approach followed by *Waelbroeck et al.* [1995] for dating the ice over the last two climatic cycles (Figure 2). Starting from the existing glaciological timescale, these authors correlate the precession and obliquity component of the deuterium record with those in the insolation, assuming a constant lag (3 ± 3 kyr) of δD with respect to 65°N mid-June insolation in the precessional band. Applying exactly the same approach, we have derived an orbitally tuned gas timescale using the $\delta^{18}O_{atm}$ record, assuming, as in the work of *Petit et al.* [1999], a correspondence between midpoint transition of $\delta^{18}O_{atm}$ and insolation maximum (Figure 3). This corresponds to an average lead of insolation with respect to - $\delta^{18}O_{atm}$ of 5.5 kyr.

Figure 4 shows the difference between these orbitally tuned timescales (OTT-ice and OTT-gas) and the GT4 glaciological timescale (for ice and gas, respectively). In both cases the differences with GT4 are small for the first 2700 m (marine stage 7.5) of the core (less than 5 kyr) but increase above 10 kyr around 3000 m (marine stage 9.1). To directly compare OTT-ice and OTT-gas, we have derived a gas timescale subtracting from OTT-ice the Δage calculated for GT4. The bottom curve of Figure 4 gives the difference between this gas age timescale and OTT-gas. For some depth intervals, this difference is large (absolute value of up to 3000 years) and significantly exceeds the expected uncertainty on Δage (1 kyr or so, including the assumption of instantaneous temperature diffusion in the firn). This is representative of the limitation of the orbital dating method resulting from both uncertainties attached to its assumptions (in particular, the assumption of constant phase between insolation change and the Vostok record) and inaccuracies in its application (e.g., filtering and peak recognition).

The strong similarities between the $\delta^{18}O_{atm}$ record and the insolation [*Jouzel et al.*, 1996; *Petit et al.*, 1999] allow defining control doors for approximately each precessional cycle for the gas timescale. We do the same for the ice timescale except for parts of the deuterium record such as stage 6 over which precessional cycles are not clearly defined. In most experiments we use Gaussian doors; that is, the likehood function associated with a given solution (see Appendix A) accounts for the width of the door defined using a Gaussian function with a width of ± 6 kyr at midheight. Importantly, the use of doors instead of fixed control points implies that we no longer impose a constant phase between either $\delta^{18}O_{atm}$ or deuterium with insolation. We realize that the use of Gaussian doors (which are well adapted from a mathematical viewpoint), even if large, could bias the solutions toward the center of the doors. To evaluate this potential bias, we performed a series of experiments with rectangular doors (total width of 12 kyr). In this case, any solution passing through a door has the same likehood, whereas it is eliminated if it passes outside the door. The results (see section 5) are quite insensitive to the shape of the doors, which gives confidence in the information we infer on the phasing between insolation and Vostok records. Moreover, we do not strictly impose the mean phases, τ_{ice} and τ_{gas}, respectively, which are open parameters of the inverse method. We just impose that these mean phases are the same as those that are supposed to construct the orbitally tuned timescales, with a Gaussian uncertainty of 3 kyr (1σ).

Additional independent information is available for the last 7 kyr of the Vostok ice core which has been dated by matching cosmogenic production rates of beryllium 10 and carbon 14, which can be reconstructed by the dendrochronology [*Raisbeck et al.*, 1998]. We use here one control point from

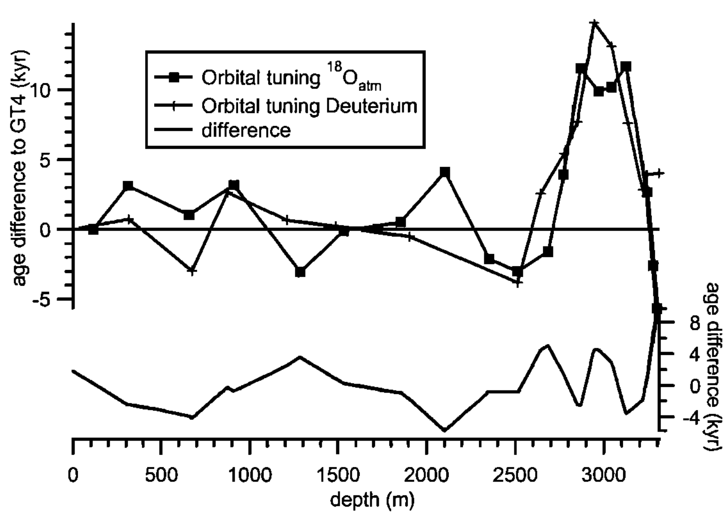

Figure 4. (top) Comparison of GT4 and the orbitally tuned chronologies based on the δD and $\delta^{18}O_{atm}$ records. Results are expressed in difference with respect to the GT4 chronology (i.e., GT4-ice for the δD tuned chronology and GT4-gas for the $\delta^{18}O_{atm}$ tuned chronology). (bottom) Difference between the two curves of the top panel.

Table 1. Chronological Information (Gaussian Control Doors) Used in the Inverse Experiments[a]

	Depth (m)	Age (kyr BP)	Uncertainty (kyr)
Fixed ice control points	178	7.179	0.1
	600	40	3
Orbital ice control points	675	40.2	6
	1211	87.6	6
	1904	132.4	6
	2516	200.6	6
	2777	246	6
	2945	293.6	6
	3134	336.2	6
	3218	373.8	6
Orbital gas control points	311	13.7	6
	909	60.7	6
	1529	105.3	6
	2104	152.9	6
	2353	177.5	6
	2686	220.5	6
	2870	267.5	6
	3044	312.1	6
	3245	385.3	6

[a] For the second experiment, we have only kept the control points for depth between 0 and 2700 m.

this timescale located at 178 m, and with an assigned age of 7179±100 years (Table 1).

Other sources provide chronological information about the Vostok core. First, we have explored the possibility of using the layer counting chronologies derived in high accumulation sites from Greenland (GRIP and GISP2) and Antarctica (Byrd) and transferred to Vostok via the correlation of atmospheric records of global significance, either methane [*Blunier et al.*, 1998] or $\delta^{18}O_{atm}$ [*Bender et al.*, 1994b, 1999]. However, this leads to inconsistencies that are difficult to explain, and rather to use this information, we discuss a posteriori the comparison between the Vostok chronology and the chronologies of the other ice cores. Second, there are indications that the ^{10}Be peak discovered at a depth of about 600 m at Vostok [*Raisbeck et al.*, 1987] is coeval with the Laschamps magnetic event [*Baumgartner et al.*, 1998], whose age is estimated at around 40 kyr BP (*Schramm et al.* [2000], for a recent review). Also, we use a Gaussian door of 40 ± 3 kyr for this depth. Third, *Basile* [1997] has identified at 1996 m an ash layer that should correspond to a volcanic eruption (Mont Berlin, Mary Byrd Land) independently dated at 141 ± 7 kyr BP by an Ar^{40}/Ar^{39} method [*Basile*, 1997]. As the correspondence has not been firmly verified, we will not use this dated depth as prior information for the inverse method, but we will compare it a posteriori to the reconstructed confidence interval.

4. The inverse method

Intuitively, an inverse method consists in finding the values of the poorly known input model parameters, while the model fits, as well as possible, a set of "observations." Here we search for the accumulation and ice flow parameters which give the best fit with respect to the available chronological information. There are nine adjustable parameters. As mentioned above, two (α and β) are used for defining the relationship between temperature and δD and three (a, b, and c) for linking the accumulation to its spatial origin with a constraint on the Ridge B accumulation rate. Two are related to ice flow, i.e., the freezing rate above the Vostok Lake ($-m_1$) which we constrain to vary between 0 and 4 mm/year and the melting rate upstream of Vostok (m_2). The last two parameters to be determined by the inverse method are the mean phases between δD and insolation (τ_{ice}) and between $\delta^{18}O_{atm}$ and insolation (τ_{gas}).

4.1. Likelihood Function

Tarantola [1987] has established a complete and fundamental mathematical theory of inverse problems on the basis of probability notions. It allows to objectively define a likelihood function (or more precisely the posterior density of probability) which measures the deviation of the model results with respect to prior information. The likelihood function is the conjunction of different sources of prior information, which constrain the inverse problem (see Appendix A). If the prior densities of a priori information are independent, the posterior density of probability on the vector of open parameters is thus just the product of these prior densities, times a normalization constant k. In practice, the normalization constant has no influence on the results given by the Metropolis-Hastings algorithm (see below) and we have taken k=1. This density of probability includes all the information we have on open parameters accounting for the physical (accumulation and ice flow) and chronological constraints. It combines not only the marginal density of probability on each open parameter separately (a, b, c, α...) but also, for example, the covariance between any pair of them. The associated posterior densities of probability on the ice and gas chronologies are given by a general formula (Appendix A), and will be statistically reconstructed by the Metropolis-Hastings algorithm described below.

4.2. Metropolis-Hastings Algorithm

The direct use of the likelihood function (equation (1)) needs the systematic exploration of the whole space of parameters. Exploring the full range of parameters at high resolution is a time-consuming problem. The use of a Monte-Carlo sampling, here the Metropolis-Hastings algorithm (MH), allows to circumvent this time problem by an efficient exploration of the space. Moreover, this algorithm is adapted for a direct computation of all the statistical quantities of interest, such as the marginal densities of probability.

The Metropolis-Hastings algorithm (Appendix B) is an iterative process, which explores the space of open parameters with a random walk, according to an acceptance-rejection rule [*Hastings*, 1970; *Metropolis et al.*, 1953]. This algorithm has recently been used in the environmental context by [*Guiot et al.*, [2000]. The suite of parameters constructed by the algorithm converges after several thousands of iterations. Here we present and discuss several inverse-modeling experiments, which differ in the choice of the chronological constraints. For each of them, we have performed three independent series of 20,000 iterations which provide very similar results, ensuring that such a number of iterations is sufficient to reach a robust solution. The information inferred by the inverse method, i.e., the posterior density of probability, is directly obtained by a statistical study of the set of parameters selected by the algorithm and is expressed in terms of density of probability using histograms. For clarity, we have computed the mean and the standard deviation for each quantity of interest, such as ice age or gas age at a given depth, or surface temperature for a given deuterium content. Importantly, this method is also appropriate for general non-Gaussian probability densities and can, for example, be applied with doors of rectangular shape.

5. Results

Our first experiment uses the prior chronological information summarized in Table 1. The chronological constraints are defined with Gaussian doors with a width of 0.1 kyr for the Holocene point (ice ages derived from the comparison between ^{10}Be and ^{14}C), 3 kyr for the ^{10}Be peak and of 6 kyr for the control doors defined from the δD (ice age) and $\delta^{18}O_{atm}$ profiles (gas age). The average phase between Vostok records and insolation is let open. We have considered that for every precessional cycle, δD and $\delta^{18}O_{atm}$ control doors are approximately independent. Although these doors are very large, we are aware that the large number of them (which results from our simple assumption that we can correctly count the number of precessionnal cycles) could place too many constraints on the inversion. In this line, we performed experiments in which one of every two doors is alternatively suppressed.

The results of this first experiment are shown in Figure 5 together with the prior chronological information used. The "best guess" timescale, i.e., the simulation with the maximum likelihood, is unable to account for the prior chronological information for the lower part of the core (below around 2700 m). The difference between the imposed mean age and the calculated value may be up to 10 kyr, largely exceeding the width of the control doors. Indeed, we derive something similar to what we previously observed for GT4 (see table of *Petit et al.* [1999]); that is, the glaciological timescale is too young for marine stages 6 and 7 and too old for stages 8 and 9. This shows that even with our modified formulation, we cannot obtain a good fit between the glaciological timescale and the orbital constraints over the entire Vostok record. Indeed, the difference between mean imposed and best guess ages varies from large negative values (- 8 kyr at 2700 m) to large positive values (+ 6 kyr at 2850 m) over a short depth interval (150 m), suggesting that something has changed abruptly around this period.

We have also explored other ways of parameterization of the basal sliding and melting. This abrupt transition appears at a depth of ~2700 m, for which the ice originates from approximately 80 km far from Ridge B. Although the base is supposed to be cold in this area (no melting and no sliding), we have tested the possibility of an abrupt change of basal conditions. However, it still appears impossible to accommodate for the orbital constraints described above. This is because even large changes in ice flow parameters only result in very smooth changes in the thinning profile. Indeed, the only way to reconcile the glaciological and orbital

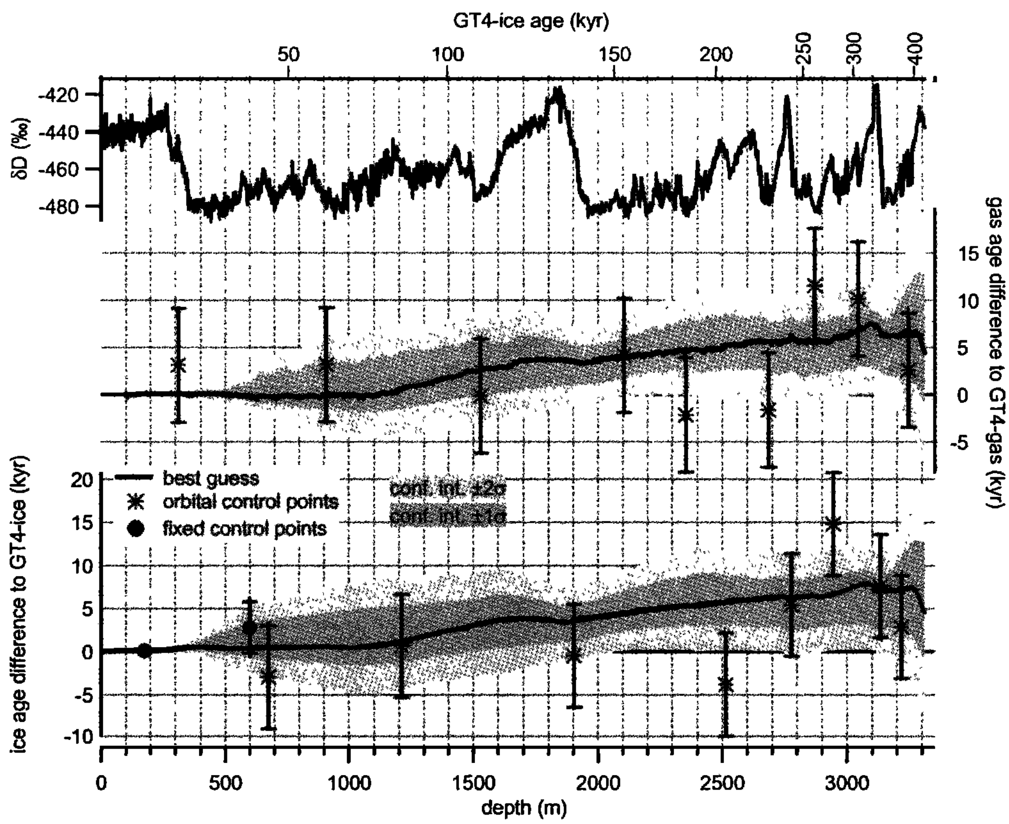

Figure 5. Chronology reconstructed by the inverse experiment applied on the whole Vostok core. (bottom) Ice age difference to the GT4-ice time scale. (middle) Gas age difference to the GT4-gas timescale. The chronological anchor points are also plotted in the figure. In fact, just the relative positions of orbital control points are assigned but not the vertical shift of all of them. (top) Deuterium record is also plotted for comparison.

approach is to assume that there exist two different regimes of accumulation along the Ridge B–Vostok axis. This is somewhat suggested by the deuterium-excess profile which shows different spectral characteristics for the last two climatic cycles than for the two previous ones, which could be explained by a different oceanic origin of the precipitation [*Vimeux et al.*, this issue]. This suggestion, however, needs confirmation and this could come in the future from close examination of aerosol fallout records, which are influenced by accumulation, such as those of sodium and beryllium 10.

One characteristic of our formulation of the inverse problem is that it cannot provide reliable results when the modeling uncertainties are no longer negligible with regard to the uncertainties associated with prior information (Appendix A). This is the case for the lower part of the core, as demonstrated by the first experiment. We thus performed a second experiment focusing on the first 2700 m of the core for which model uncertainties are much smaller. We no longer account for prior chronological information below 2700 m. For this experiment, the best guess dating is consistent with prior imposed information (Figure 6), and this new reconstruction can be fully interpreted as far as the ice and gas timescales are concerned. In addition to the best guess dating, this figure shows the confidence interval of our reconstruction (mean ± 1σ). These results are practically not affected (by less than 1 kyr) for other experiments, i.e., neither when Gaussian doors are replaced by rectangular doors or when one of every two doors is suppressed.

Our "best guess" chronology is slightly older than GT4 for the last climatic cycle; the difference reaches 2.5 kyr for the ice and 2 kyr for the gas. This is principally due to the use of the ^{10}Be peak control point defined above, which was not used to define the GT4 timescale. We have performed another experiment without this peak (not shown here), and for this experiment, both the best guess and the confidence interval are in better agreement with GT4.

The confidence interval of the inverse dating is ~0.1 kyr (1σ) for the end of the Holocene, and increases up to ~3 to 4 kyr (Figure 6). Within this accuracy, the age of the volcanic ash observed at 1996 m (141±7 kyr BP) is fully consistent with the glaciological confidence interval age at this depth: 142.1±2.6 kyr BP (1σ). The glaciological age of the ^{10}Be peak (39.4±2 kyr BP) is consistent but slightly younger than that supposed a priori (40±3 kyr).

We can notice that for the upper 500 m of the record, the uncertainty is less important for the gas age than for the ice age. This difference between ice and gas is due to two compensating effects: a decrease in temperature induces a smaller accumulation, and thus an older ice age, but it also induces an increase in Δage. Thus the gas age is relatively unchanged, which shows that our modeling hypotheses strongly constrain the gas dating down to ~500 m (i.e., over the last 20 kyr or so).

We now compare our inverse experiment with respect to datings of other ice cores both from Antarctica and Greenland, examine the constraints that the inverse method provides on the deuterium-temperature relationship and on the spatial variation of accumulation and then discuss the phase of δD, and $\delta^{18}O_{atm}$ with respect to insolation.

5.1 Comparison With Other Ice Core Datings

Various approaches based on the use of atmospheric CH_4 [*Blunier and Brook*, 2001; *Blunier et al.*, 1998] and $\delta^{18}O_{atm}$ [*Bender et al.*, 1999] records of global significance, or global time markers such as the ^{10}Be peak around 40 kyr BP [*Yiou et*

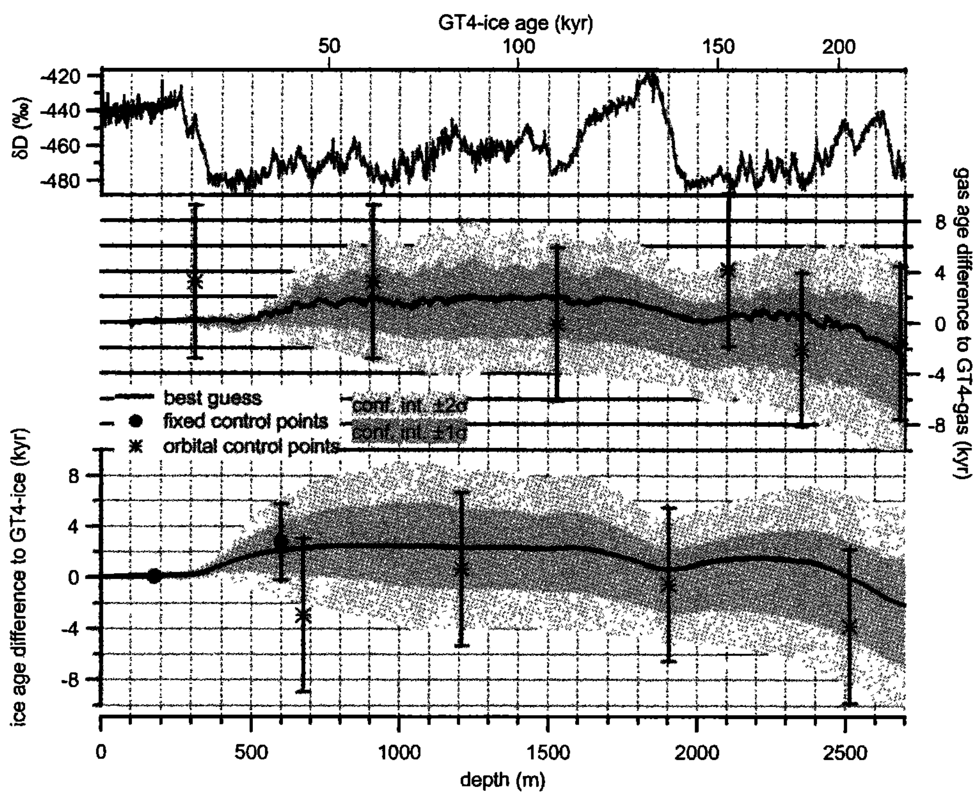

Figure 6. Same as Figure 5 for the upper 2700 m of the Vostok core and for the second experiment.

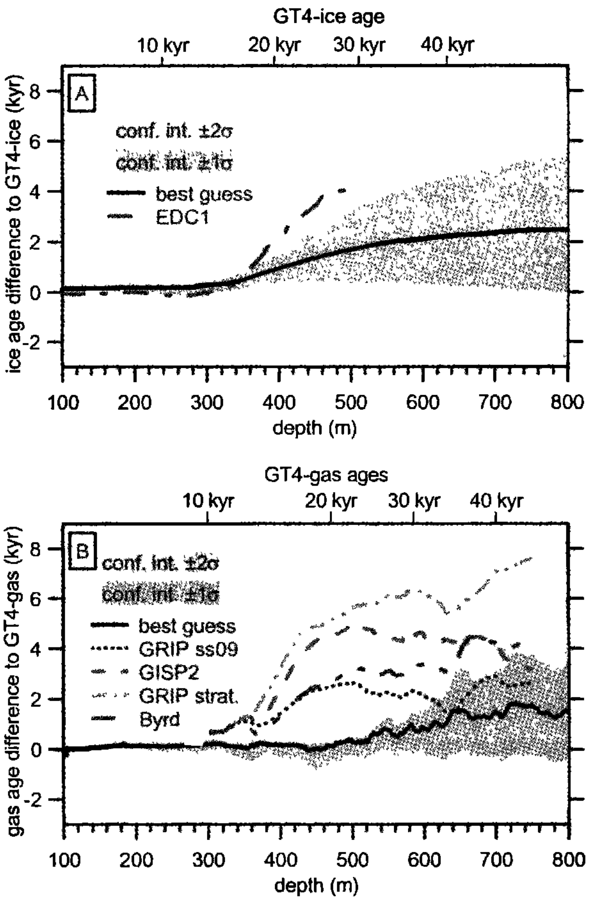

Figure 7. Comparison of the best guess and confidence interval reconstructed by the inverse method with other ice core chronologies. (A) The Dome C ice chronology transported on the Vostok depth via ash layers correlation. (B) The GRIP (by layer counting and modeling), GISP2, and Byrd gas chronologies transported to the Vostok depth via methane correlation. Ages are expressed in differences with respect to the GT4 (ice and gas, respectively) timescale.

al., 1997], can be used to correlate ice cores from southern and northern hemispheres. On the basis of the correlation made by *Blunier et al.* [1998] using the CH_4 record, we have compared the gas chronologies of ice cores from Greenland (GRIP and GISP2) and Antarctica (Byrd and Vostok) for the last 45 kyr (Figure 7). We have also compared the ice chronologies of Vostok and Epica Dome C with the correlation of volcanic horizons. GRIP, GISP2, and Byrd are dated by annual layer counting [*Alley et al.*, 1997; *Hammer et al.*, 1994, 1997a, 1997b], whereas ice flow and accumulation modeling has been applied to GRIP [*Dansgaard et al.*, 1993] and to EPICA Dome C [*Schwander et al.*, 2001]. All the datings are in excellent agreement as far as the last 13 kyr are concerned. They start to diverge during termination I, and large differences appear during the late glacial. The GRIP modeling, Byrd, and EPICA Dome C ice cores chronologies differ by less than 1 kyr. Instead, with respect to those three chronologies, the GRIP and GISP2 stratigraphies are older by up to ~2 kyr, whereas the Vostok GT4 and chronology is younger by up to ~3 kyr. Even accounting for its uncertainty, the inverse chronology is younger than the stratigraphic datings from GRIP and GISP2.

We now examine if this disagreement could be explained by possible incorrect hypotheses in our modeling approach. The Pimienta-Barnola firn model [*Barnola et al.*, 1991] has empirically been adjusted with modern data, and results have been extrapolated to the glacial part at Vostok for temperature and accumulation that do not presently exist anywhere in Greenland or Antarctica. Recently, more physical models have been established with different hypotheses [*Arnaud et al.*, 2000], and their estimation of Δage are always smaller than that estimated by the Pimienta-Barnola model. The difference can reach ~800 years for glacial conditions and with temperature and accumulation used to construct the GT4 timescale; this difference is accentuated if we examine scenarios with colder temperatures and smaller accumulation rates. Our study thus argues for these new more physical firn models. This could, but only partially (i.e., by a maximum of ~ 1.5 to 2 kyr), reconcile the Vostok and other deep ice core chronologies.

We can also suspect that this difference results from the method we have used to model the accumulation (i.e., the use of second order to parameterize the spatial accumulation and the T_i-accumulation or δD-T_i relationships). However, because of compensating effects, the gas age is quite insensitive to those formulations between 20 and 30 kyr BP, a period over which the chronologies already diverge. Indeed, whatever the parameterization of accumulation that we take, a reduced accumulation induces an older ice chronology, but also a larger Δage, leading to an almost unchanged gas chronology. Overall, this makes it very unlikely that the difference between our "best guess" chronology and other chronologies results from an incorrect estimate of Vostok accumulation changes. Finally, there are no large uncertainties on the thinning function down to this depth (the first 600 m of the Vostok core). To sum up, our inverse method to date the Vostok core clearly pleads for the use of more physical models to evaluate the gas age–ice age difference and is in better agreement with the glaciological timescales derived for GRIP and EPICA Dome C and with the Byrd chronology than with the GRIP and GISP2 stratigraphic datings for the glacial part (i.e., between ~ 20 and 50 kyr BP).

5.2 Reconstruction of Past Temperature and Accumulation

Another interesting application of the inverse method to the glaciological dating model is the reconstruction of the deuterium-temperature relationship. Indeed, the above prior chronological information can constrain this relationship (Figure 8). The degree of validity of our inverse reconstruction depends of the modeling hypotheses that we have made, in particular, we have assumed that accumulation is proportional to the derivative of the saturation water vapor pressure at the temperature of snow formation. If this law is verified, our results indicate that a δD change of 50 ‰ (roughly corresponding to the full range of variations observed in the Vostok core), corresponds to a change in surface temperature (Ts) of 10.9 ± 2.2°C (1σ). For such a change in δD the current interpretation [*Jouzel et al.*, 1993, 1987; *Petit et al.*, 1999], based on the use of the present-day spatial slope (6.04‰/°C) and including a correction for the isotopic change of seawater (~10 ‰), gives an estimate also close to 10°C. The current interpretation is thus consistent with the temperature changes inferred from the inverse method (Figure 8). We indeed now better understand from climate and isotopic models why the situation differs between Greenland, where temperature is

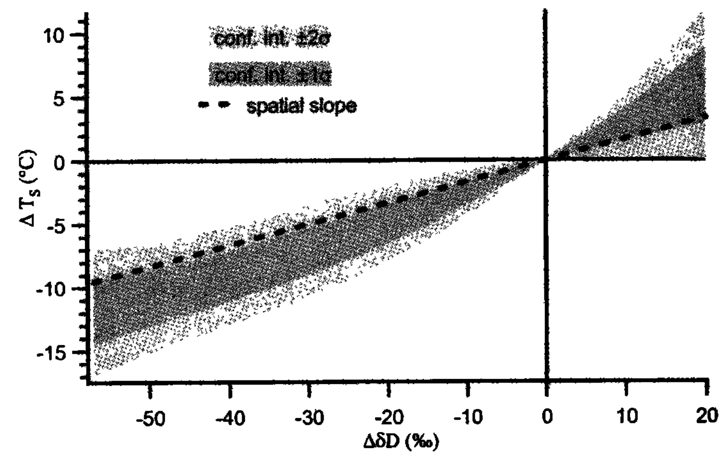

Figure 8. Deuterium-temperature relationship reconstructed by the inverse experiment.

underestimated by up to a factor of 2 using the classical isotopic approach, and Antarctica. In Greenland there are large glacial-interglacial changes in precipitation seasonality which should be taken into account when interpreting the isotopic signal [*Krinner et al.*, 1997; *Werner et al.*, 2000], whereas Antarctic precipitation is much less affected by seasonality [*Delaygue et al.*, 2000; *Krinner et al.*, 1997]. In addition, glacial-interglacial changes in the origin of the precipitation appear to have little influence on the associated isotopic shift in central Antarctica [*Delaygue et al.*, 2000].

The inverse method also gives information about the spatial change of accumulation between Ridge B and Vostok. Because of the use of precise prior dating of the Holocene, accumulation near Vostok is well constrained: 2.06 ± 0.05 cm of ice/year, but the accuracy decreases with the distance from Vostok. We can notice that the reconstruction is consistent with the linear profile that is used to define the GT4 timescale. However, differences would be larger if one took into account the orbital constraints over the entire 400 kyr period. This, as mentioned above, may require a different formulation of the spatial accumulation change with two regimes of accumulation between Vostok and Ridge B.

5.3 The Timing of $\delta^{18}O_{atm}$ and δD Variations With Respect to Insolation

Although our dating method uses chronological information retrieved from orbitally tuned series, the derived control points have an associated error of ± 6 kyr (>1/4 of precessional period) and only poor assumptions are made on the phase lag between Vostok records and the insolation. As explained in the description of the method, the mean phase between δD or -$\delta^{18}O_{atm}$ and insolation is not imposed in our chronological approach but deduced from the inverse experiment. Therefore in contrast to orbitally tuned chronologies such as those presented in Figures 2 and 3, our "best guess" experiment is an optimized glaciological timescale that bears information on the dynamics of the climatic response.

Moreover, as mentioned earlier, one major advantage of the present inverse dating method is the determination of

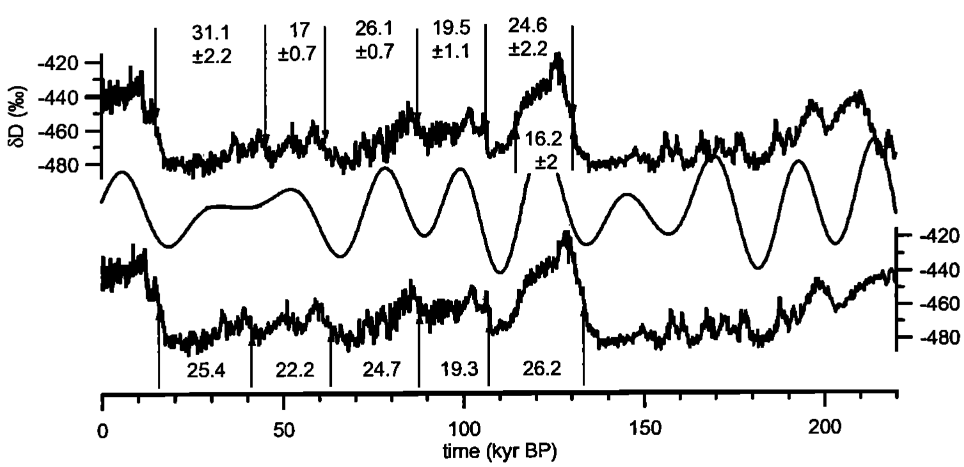

Figure 9. Comparison of Vostok δD record dated either with the "mean" glaciological chronology for the ice (top) or with the orbitally tuned timescale based on deuterium record, OTT-ice (bottom). For each precessional cycle, we compare the durations established with the glaciological time scale (confidence interval reconstructed by the inverse method) and with the orbital time scale. For reference, insolation (21 June, 65°N) have been plotted on the figure, with a shift of –5.5 kyr corresponding to the phase supposed to construct the orbital timescale.

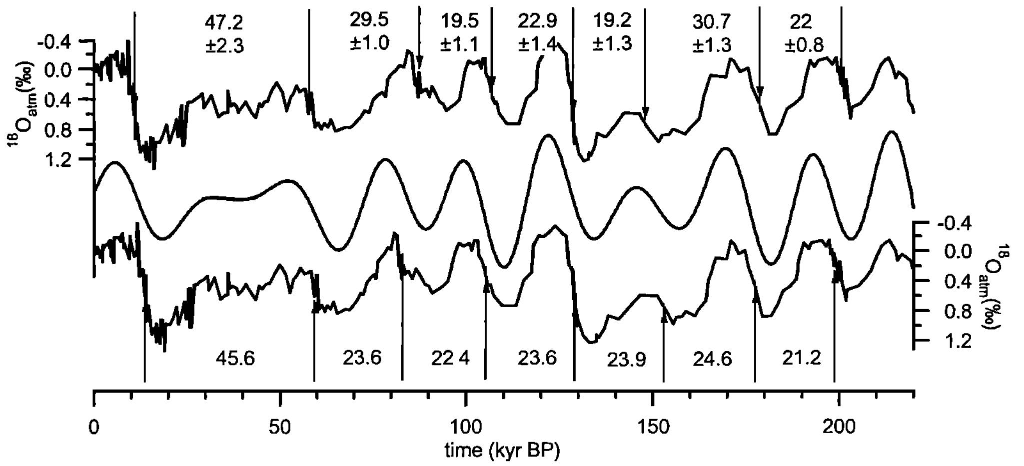

Figure 10. Comparison of Vostok $\delta^{18}O_{atm}$ record dated either with the "mean" glaciological chronology for the gas (top) or with the orbitally tuned timescale based on deuterium record, OTT-ice (bottom). For each precessional cycle, we compare the durations established with the glaciological timescale (confidence interval reconstructed by the inverse method) and with the orbital timescale. For reference, insolation (21 June, 65°N) has been plotted in the figure, with a shift of –3 kyr corresponding to the phase supposed to construct the orbital timescale.

confidence intervals, not only on the ages themselves but also on the duration of given events. Because our inverse reconstruction is inherently consistent with glaciological flow laws, the uncertainty on the age difference between two neighboring levels is much lower than the uncertainty on each level's age. We can thus evaluate with a high degree of precision how the phase lag between the $\delta^{18}O_{atm}$ and the insolation (or between the δD and the insolation) evolves along the Vostok ice core. To analyze the changing phase of δD, we compare the duration of the precessional cycle deduced from the orbital timescale (OTT-ice and OTT-gas, respectively) and deduced from the inverse experiment (Figures 9 and 10, respectively). This phase lag does, indeed, significantly vary with time: over the last two climatic cycles, the phase lag between $\delta^{18}O_{atm}$ or δD and insolation varies for several thousands of years, and it is larger in full glacial conditions.

Is this pattern an artifact of the dating method or a climatic signal? The glaciological model assumes that the physical properties of the ice remain constant along the whole core. The climatic variations are taken into account through the changes in accumulation and surface temperature only. Therefore if the ice ductility or viscosity actually vary along the core due to changes in dust content, this could create biases in the "best guess" chronology calculation. However, high dust content makes the ice harder for compression but softer for shear [*Dahl-Jensen et al.*, 1997], and it seems that the difference in thinning could only be observed locally (microfolds or boudinage), but on the average, the ice must obey the glaciological thinning rate. Moreover, our modeling of accumulation may have an influence on our reconstructed event duration. Indeed, cold stages (MIS 2 and 4 and 6) correspond to intense atmospheric circulation and dry atmosphere (ice with high dust content), which may have an influence on accumulation rate. However, there is not a systematic shift in the estimation of cold stage duration: MIS 2 and 4 are longer in glaciological timescale than in orbitally tuned timescale, whereas it is the contrary for MIS 6. We can also suspect the definition of our chronological constraints. With this in mind, we have performed several tests of sensibility, with either "rectangular door" instead of "Gaussian door," or with a perturbed position of the middle of these doors. However, in all these experiments, our results are qualitatively unchanged.

In conclusion, the variation in lag between $\delta^{18}O_{atm}$ or δD and insolation may thus be a real feature of the climate system. This has several important implications.

1. We present here the first quantitative assessment of the variation in the phase lags or leads between a climatic record and insolation. This is a measure of the error induced by the assumption of constant phase between the climatic response and the insolation in orbitally tuned timescales, such as the marine SPECMAP timescale. The phase lags between $\delta^{18}O_{atm}$ or δD and insolation may vary by more than 5 kyr for two successive precessional cycles. These variations of phase represent the portion of the total error on orbitally tuned chronologies that results from the constant phase hypothesis. The change of phase between $^{18}O_{atm}$ and insolation could be partly biased by the phase lag of $^{18}O_{atm}$ with respect to $^{18}O_{sw}$, which may be larger [*Leuenberger*, 1997] than previously supposed [*Bender et al.*, 1994b]. As the phase between the climatic response and the orbital forcing would be constant if the climate system were simply linearly responding to variations in insolation, our results give a measure of the nonlinear character of the climate system.

2. The variation in the phase lags do not seem to be randomly distributed: the lags between $\delta^{18}O_{atm}$ or δD and insolation increase during glacials (i.e., between 75 and 17 kyr BP, MIS 4 to 2; and between 180 and 133 kyr BP, MIS 6). Therefore, our results seem to indicate that the climatic response to the insolation forcing is of a different nature during glacials than during interglacials. This confirms *Paillard*'s [1998] model in which the climate system is characterized by three distinct states depending on the amount of ice stored on the continents (i.e., interglacial, "mild glacial," and "full glacial" regimes).

3. Finally, the last interglacial dated by the glaciological model is impressively long as previously suggested [*Jouzel et al.*, 1993, 1996; *Lorius et al.*, 1985; *Petit et al.*, 1999]: 16.2 ± 2

kyr from 133.4 to 117.2 kyr BP at mid transition. The age at mid transition (termination II) is, however, significantly younger than that of 139 kyr BP derived in the initial dating of *Lorius et al.* [1985]. This initial Vostok timescale has recently been supported by a dating of the penultimate deglaciation in a deep-sea core record from the Bahamas [*Henderson and Slowey*, 2000], which places the midpoint age for the penultimate deglaciation at 135± 2.5 kyr BP, 7 kyr earlier than assigned in the SPECMAP dating. Our inverse method rules out the possibility of a Vostok midtransition as old as 139 kyr BP even accounting for our estimated uncertainty of ± 2.5 kyr. Indeed, the *Lorius et al.* [1985] timescale was based on the assumption of a constant accumulation between Vostok and Ridge B (equals to the one of Vostok) which has been shown later to be very unlikely [*Jouzel et al.*, 1993]. On the other hand, our dating places the $\delta^{18}O_{atm}$ mid transition at 128.6 ± 2.6 kyr. This would be in relatively good agreement with the SPECMAP chronology, which places the mid deglaciation at 128 kyr BP if we assume that this $\delta^{18}O_{atm}$ transition is largely driven by the glacial-interglacial of the seawater $\delta^{18}O$ and accounts for the fact that $\delta^{18}O_{atm}$ lags the seawater $\delta^{18}O$ by about 1 kyr [*Bender et al.*, 1994b]. On the other hand, a recent compilation of published high-quality U-Th dates (i.e., with initial $^{234}U/^{238}U$ ratios close to the present-day seawater $^{234}U/^{238}U$ ratio) of the last interglacial high sea level stands [*Balbon*, 2000] indicates that marine stage 5e probably extended from 119 to 128 kyr BP. This would place the corresponding midtransitions at ~ 116 (5e to 5d) and 130 kyr BP (6 to 5e) with stage 5e having a duration (14 kyr) relatively close from that predicted by the glaciological approach for the last interglacial at Vostok.

6. Conclusion

The objective of the present study was to constrain, with an appropriate inverse method, the Vostok glaciological dating model with available chronological information. Indeed, poorly constrained accumulation or ice flow parameters such as the δD-T_S relationship, the spatial variation of accumulation upstream Vostok, or the melting rates at the bottom of the ice sheet are the cause of large dating uncertainties except if a priori chronological information is used. To constrain these accumulation and ice flow parameters, we have assigned ages at certain depths with their associated uncertainties (Gaussian doors). We use the absolute chronology derived over part of the Holocene from the comparison of the ^{10}Be profile with the ^{14}C record [*Raisbeck et al.*, 1998], chronological information linked to the ^{10}Be peak and orbitally derived control doors. These large doors (± 6 kyr) are defined simply assuming that we can correctly count the number of precessional cycles in the δD and $\delta^{18}O_{atm}$ Vostok records but with no strict assumption on the mean phase between those records and the insolation changes. The inverse method then consists in finding the parameter values that best fit this chronological information. In doing so, we not only provide an optimized glaciological timescale and its associated uncertainty but also reliable estimates of the duration of climatic events and constraints on the various model parameters. Also, as the phase relationship between Vostok records and insolation is not strictly imposed, our approach bears information on the dynamics of the climatic response which were accessible, neither from an orbitally tuned timescale (with imposed phases), nor from previously defined Vostok glaciological timescales (with fixed control points). The main results of our study are the following:

1. Our "best guess" chronology is slightly older than GT4 for the first 2500 m of the ice core (~200 kyr), and the difference reaches 2.5 kyr at maximum. For the last two climatic cycles, glaciological chronologies are in relatively good agreement with orbitally tuned chronologies. For older periods, a good fit is possible only if we assume two different accumulation regimes between Vostok and Ridge B, but this needs to be confirmed. The comparison of our results with other ice core datings shows that the stratigraphic chronologies of Greenland are older than our "best guess" chronology. This difference could only partly be explained by an overestimation of the Δage by the semiempirical firn model used here.
2. Our inverse method supports the interpretation of δD or $\delta^{18}O$ in ice assuming that the present-day spatial slope can be taken as a surrogate of the temporal slope as currently proposed for Antarctic cores. This result, however, depends on the approach adopted for modeling the accumulation change (assumed to be proportional to the derivative of the water vapor pressure at the temperature of snow formation).
3. This inverse method allows the first assessment of the evolution of the phase between Vostok climatic records and insolation. We show that the phase lags (with respect to the June 21 insolation at 65°N) seem to vary significantly with time, thus giving a measure of the nonlinear character of the climate system. These variations do not seem randomly distributed, suggesting that the mechanisms linking the climatic response to the insolation forcing are of a different nature during glacials than during interglacials.
4. We confirm that the last interglacial as recorded in the Vostok δD record (16.2 ± 2 kyr) is significantly longer than half precessional cycle (~11 kyr), extending from 133.4 (± 3) to 117.2 (± 3) kyr BP at midtransition.

Our study illustrates the potential of applying inverse methods for dating purposes and how this provides other interesting paleoclimatic information related either to temperature reconstruction or to climate mechanisms. The approach should be easily extended to other problems such as the interpretation of isotopic anomalies recorded in ice cores (influenced both by temperature and by accumulation) or the correlation between different ice cores in which chronological information are contained both in the ice and in the entrapped air bubbles. As far as the Vostok dating presented here is concerned, it appears that a large source of uncertainty lies in the lack of accumulation data upstream Vostok. This highlights the need for surface snow isotopic and accumulation measurements along a Vostok-Ridge B transect. Also, it will be interesting to apply this inverse modeling to sites located on domes, where the parameterization of the accumulation should be simpler, such as Dome F where an ice core covering three climatic cycles has been recently retrieved [*Dome F Ice Core Research Group*, 1998] and Dome C where the EPICA (European Project for Ice Coring in Antarctica) drilling program to reach the bedrock is being conducted.

Appendix A: General Formulation of Inverse Problem

Let us consider a model, which is mathematically defined as a function $G: M \rightarrow D$. M is the space of input parameters vector of the model, and for each $m \in M$, the model G associates an output parameters vector $d=G(m) \in D$. Let us suppose that with methods independent of the model G, for example direct measurements or indirect estimates, we have access to an independent information on d. This prior information is mathematically translated by a prior density of probability $\rho^D(d)$ on D. This density could be, for example, of Gaussian or lognormal type, or more generally multimodal. Symmetrically, we can have an estimate, perhaps with a large uncertainty, of the input parameters vector, which gives access to a prior density of probability $\rho^M(m)$ on M. Intuitively, the estimate of m gives, through model G, an estimate of d; and symmetrically, the estimate of d gives access to information on m through the model. An inverse problem tries to respond to the following question: how to infer the optimal information from (1) the estimate of d, i.e., $\rho^D(d)$; (2) the estimate of m, i.e., $\rho^M(m)$; and (3) the relation between m and d given by the model G. This optimal information is called posterior information, and is mathematically translated by two posterior densities of probability $\sigma^M(m)$ on M and $\sigma^D(d)$ on D [*Tarantola*, 1987], given by

$$\sigma^M(m)=\rho^M(m)\frac{\rho^D(G(m))}{\mu^D(G(m))},$$

$$\sigma^D(d)=\frac{\rho^D(d)}{\mu^D(d)}\int_M \delta(d-G(m))\rho^M(m)dm,$$

where $\mu^M(m)$ ($\mu^D(d)$, respectively) is the homogeneous, or noninformative, probability density on M (D respectively). Importantly, this mathematical formulation of inverse problems assumes that the model is perfect, and we only doubt the parameter's values. In practice, a model is never perfect and the condition for using this formalism is that model uncertainties are negligible with regard to prior uncertainties on model input and output parameters. However, we have to keep in mind that if it is not the case, this formalism is not usable. A more general formalism has been established to take into account the modeling uncertainties [*Tarantola*, 1987], but first, it complicates the practical resolution, and second, it is, in general, not easy to evaluate the model uncertainties.

Concerning the practical resolution of equation (a) and (b), we can analytically solve this inverse problem only in special cases. The case most known is the linear problem with Gaussian uncertainties and has been extensively studied [e.g., *Tarantola*, 1987]. When the model is a general nonlinear one, the practical resolution needs an exploration of the space of model input parameters M, and these methods are called Monte Carlo methods. A good way for exploring the space M is to use an algorithm that is able to construct a suite of sets m_1, m_2, m_3,..., which samples the posterior density of probability $\sigma^M(m)$. These methods are called Monte Carlo sampling and present several advantages. First, the exploration is made preferentially in the interesting regions of M, i.e., the regions where the posterior density is not negligible. Second, it could be demonstrated that the suite of corresponding sets of output parameters $d_1=g(m_1)$, $d_2=G(m_2)$, $d_3=G(m_3)$,..., samples the posterior density of probability $\sigma^D(d)$. Third, we have transformed our complicate probabilistic problem in a simple statistical study of the suite of parameters, because any quantity of interest such as the marginal probability densities or the covariance can be evaluated from the generated suite of runs. The Metropolis-Hastings algorithm is an example of Monte Carlo sampling and is described in Appendix B.

Appendix B: Metropolis-Hastings Algorithm

Given a space X and a target density of probability $\sigma(x)$ on X, the property of the Metropolis-Hastings algorithm is to construct a suite x_1, x_2, x_3,..., $\in X$, which samples the density of probability σ. The MH algorithm browses iteratively the space X according to a random walk based on an acceptance-rejection rule [*Gelman et al.*, 1995; *Hastings*, 1970; *Metropolis et al.*, 1953]. Starting from the previous random position x_k of the parameter, the algorithm randomly chooses a neighbor x_{k+1}^{cand}, which is a candidate for being the next element of suite x_{k+1}. A random number r is then uniformly chosen between 0 and 1, and x_{k+1}^{cand} is accepted (i.e., $x_{k+1}= x_{k+1}^{cand}$) if and only if $r<\sigma(x_{k+1}^{cand})/\sigma(x_k)$. Else, we keep the previous element of the suite: $x_{k+1}=x_k$. We can remark that if $\sigma(x_{k+1}^{cand})\geq\sigma(x_k)$, which means that the candidate is most likely than the previous element, then the candidate is always accepted because $\sigma(x_{k+1}^{cand})/\sigma(x_k)\geq 1$. The choice of the candidate with respect to the previous element is done with a jump distribution J: the candidate is chosen according to the probability distribution $J(x_{k+1}^{cand}-x_k)$. A sufficient condition to ensure the convergence to the target distribution σ is that the J function was symmetric and strictly positive. It is the case when we use a multivariate Gaussian distribution. The rapid convergence of the suite largely depends of the choice of the variance-covariance matrix of this Gaussian distribution and, in practice, this matrix is updated every L iterations (typically, L=100) with regard to the observed variance-covariance matrix of the suite x_k.

Acknowledgments. This work has benefited from discussions with Joel Guiot, Valérie Masson and Dominique Raynaud. Frédéric Parrenin thanks Nicolas Caillon, Françoise Vimeux, Gilles Delaygue and Jean-Yves Peterschmitt for technical help. This work is supported by PNEDC (Programme National d'Etudes de la Dynamique du Climat). Correspondence and requests for the materials to F.P. (parrenin@glaciog.ujf-grenoble.fr).

References

Alley, R. B., et al, Visual-stratigraphic dating of the GISP2 ice core: basis, reproductibility, and application, *J. Geophys. Res.*, *102* (C12), 26,367-26,381, 1997.

Arnaud, L., J.-M. Barnola, and P. Duval, Physical modeling of the densification of snow/firn and ice in the upper part of polar ice sheets, in *Physics of Ice Core Records*, edited by T Hondoh, pp. 285-305, Hokkaido Univ. Press, Sapporo, Japan, 2000.

Balbon, E., Variabilité climatique et circulation thermohaline dans l'Océan Atlantique Nord et en Mer de Norvège au cours du stade isotopique marin 5, Ph.D. thesis, Univ. Paris XI, France, 2000.

Barnola, J.-M., D. Raynaud, Y.S. Korotkevich, and C. Lorius, Vostok ice core provides 160,000-year record of atmospheric CO_2, *Nature*, *329*, 408-414, 1987.

Barnola, J.-M., P. Pimienta, D. Raynaud, and Y.S Korotkevich, CO_2-climate relationship as deduced from the Vostok ice core: a re-examination based on new measurements and a re-evalution of the air dating, *Tellus, Ser. B*, *43*, 83-90, 1991.

Basile, I., Origine des aérosols volcaniques de la carotte de glace de Vostok (Antarctique), Ph.D. thesis, Univ. Joseph Fourier, Grenoble, France, 1997.

Baumgartner, S., J. Beer, J. Masarik, G. Wagner, L. Meynadier, and H.-A. Synal, Geomagnetic modulation of the ^{36}Cl flux in the GRIP ice core, Greenland, *Science*, *279*, 1330-1332, 1998.

Bender, M., T. Sowers, and L.D. Labeyrie, The Dole effect and its variation during the last 130,000 years as measured in the Vostok core, *Global Biogeochem. Cycles*, *8*, 363-376, 1994a.

Bender, M., T. Sowers, M.L. Dickson, J. Orchado, P. Grootes, P.A. Mayewski, and D.A. Meese, Climate connection between Greenland and Antarctica during the last 100,000 years, *Nature*, *372*, 663-666, 1994b.

Bender, M., B. Malaize, J. Orchado, T. Sowers, and J. Jouzel, High precision correlations of Greenland and Antarctic ice core records over the last 100 kyr, in *Mechanisms of Global Climate Change at Millennial Timescales*, *Geophys. Monogr. Ser.*, *112*, edited by

P.U. Clark, R.S. Webb, and L.D. Keigwin, pp. 149-164, AGU, Washington, D. C., 1999.

Blunier, T., and E.J. Brook, Timing of millennial-scale climate change in Antarctica and Greenland during the last glacial period, *Science*, *291*(5501), 109-112, 2001.

Blunier, T., et al., Asynchrony of Antarctic and Greenland climate change during the last glacial period., *Nature*, *394*, 739-743, 1998.

Caillon, N., J.P. Severinghaus, J.-M. Barnola, J.C. Chappellaz, J. Jouzel, and F. Parrenin, Estimation of temperature change and of gas age-ice age difference, 108 kyr B.P., at Vostok, Antarctica, *J. Geophys. Res.*, this issue.

Chappellaz, J., J.-M. Barnola, D. Raynaud, Y.S. Korotkevich, and C. Lorius, Ice-core record of atmospheric methane over the past 160,000 years, *Nature*, *345*, 127-131, 1990.

Dahl-Jensen, D., T. Thorsteinsson, R. Alley, and H. Shoji, Flow properties of the ice from the Greenland Ice Core Project ice core: The reason for folds?, *J. Geophys. Res.*, *102*, 26,831-26,840, 1997.

Dansgaard, W., S.J. Johnsen, H.B. Clausen, D. Dahl-Jensen, N.S. Gunderstrup, C.U. Hammer, J.P. Steffensen, A. Sveinbjörnsdottir, J. Jouzel, and G. Bond, Evidence for general instability of past climate from a 250-kyr ice-core record, *Nature*, *364*, 218-220, 1993.

de Angelis, M., M. Barkov, and V.N. Petrov, Aerosol concentrations over the last climatic cycle (160 kyr) from an Antarctic ice core, *Nature*, *325*, 318-321, 1985.

Delaygue, G., J. Jouzel, V. Masson, R.D. Koster, and E. Bard, Validity of the isotopic thermometer in central Antarctica: Limited impact of glacial precipitation seasonality and moisture origin, *Geophys. Res. Lett.*, *27*(17), 2677-2680, 2000.

Dome F Ice Core Research Group, Preliminary investigation of paleoclimate signals recorded in the ice core from Dome Fuji station, East Dronning Maud Land, Antarctica, *Ann. Glaciol.*, *27*, 338-342, 1998.

Gelman, A., J.B. Carlin, H.S. Stein, and D.B. Runbin, *Bayesian Data Analysis*, Chapman and Hall, New York, 1995.

Guiot, J., F. Torre, D. Jolly, O. Peyron, J.J. Boreux, and R. Cheddadi, Inverse vegetation modelling by Monte Carlo sampling to reconstruct palaeoclimates under changed precipitation seasonality and CO_2 conditions: Application to glacial climate in Mediterranean region, *Ecol. Model.*, *127*, 119-140, 2000.

Hammer, C.U., H.B. Clausen, and C.C. Langway, ECM stratigraphic dating of the Byrd station ice core, *Ann. Glaciol.*, *20*, 115 - 120, 1994.

Hammer, C.U., H.B. Clausen, and C.C. Langway, 50,000 years of recorded global volcanism, *Clim. Change*, *35*, 1-15, 1997a.

Hammer, C.U., K.K. Andersen, H.B. Clausen, D. Dahl-Jensen, C.S. Hvidberg, and P. Iversen, The stratigraphic dating of the GRIP ice core, Geophys. Dep., Niels Bohr Inst. for Astron., Phys. and Geophys., Copenhagen, Denmark, 1997b.

Hastings, W.K., Monte Carlo sampling methods using Markov chains and their application, *Biometrika*, *57*, 97-109, 1970.

Henderson, G.M., and N.C. Slowey, Evidence from U-Th dating against Northern Hemisphere forcing of the penultimate deglaciation, *Nature*, *404* (6773), 61-66, 2000.

Hoffmann, G., V. Masson, and J. Jouzel, Stable water isotopes in atmospheric general circulation models, *Hydrol. Proc.*, *14*, 1385-1406, 2000.

Jouzel, J., Calibrating the Isotopic Paleothermometer, *Science*, *286* (5441), 910-911, 1999.

Jouzel, J., C. Lorius, J.-R. Petit, C. Genthon, N.I. Barkov, V.M. Kotlyakov, and V.M. Petrov, Vostok ice core: A continuous isotope temperature record over the last climatic cycle (160,000 years), *Nature*, *329* (6138), 403-408, 1987.

Jouzel, J., et al., Extending the Vostok ice-core record of paleoclimate to the penultimate glacial period, *Nature*, *364*, 407-412, 1993.

Jouzel, J., et al., The two-step shape and timing of the last deglaciation in Antarctica, *Clim. Dyn.*, *11*, 151-161, 1995.

Jouzel, J., et al., Climatic interpretation of the recently extended Vostok ice records, *Clim. Dyn.*, *12*, 513-521, 1996.

Jouzel, J., J.R. Petit, R. Souchez, N.I. Barkov, V.Y. Lipenkov, D. Raynaud, M. Stievenard, N.I. Vassiliev, V. Verbeke, and F. Vimeux, More than 200 meters of lake ice above subglacial lake, Vostok, Antarctica, *Science*, *286* (5447), 2138-2141, 1999.

Kapitza, A.P., J.K. Ridley, G.d.Q. Robin, M.J. Siegert, and I.A. Zotikov, A large deep freshwater lake beneath the ice of central East Antarctica, *Nature*, *381*, 684-686, 1996.

Krinner, G., C. Genthon, and J. Jouzel, GCM analysis of local influences on ice core δ signals, *Geophys. Res. Lett.*, *24* (22), 2825-2828, 1997.

Leuenberger, M.C., Modeling the signal transfer of seawater $\delta^{18}O$ to the $\delta^{18}O$ of atmospheric oxygen using a diagnostic box model for the terrestrial and marine biosphere, *J. Geophys. Res.*, *102*, 26,841-26,850, 1997.

Lorius, C., J. Jouzel, C. Ritz, L. Merlivat, N.I. Barkov, Y.S. Korotkevitch, and V.M. Kotlyakov, A 150,000-year climatic record from Antarctic ice, *Nature*, *316*, 591-596, 1985.

Martinson, D.G., N.G. Pisias, J.D. Hays, J. Imbrie, T.C. Moore, and N.J. Shackleton, Age dating and the orbital theory of the ice ages: development of a high-resolution 0-300,000 years chronostratigraphy, *Quat. Res.*, *27*, 1-30, 1987.

Metropolis, N., A.W. Rosenbluth, M.N. Rosenbluth, A.H. Teller, and E. Teller, Equations of state calculations by fast computing machines, *J. Chem. Phys.*, *21*, 1087-1092, 1953.

Paillard, D., The timing of Pleistocene glaciations from a simple multiple-state climate model, *Nature*, *391*, 378-381, 1998.

Petit, J.-R., L. Mounier, J. Jouzel, Y.S. Korotkevich, V.I. Kotlyakov, and C. Lorius, Paleoclimatological and chronological implications of the Vostok core dust record, *Nature*, *343*, 56-58, 1990.

Petit, J.R., et al., Climate and atmospheric history of the past 420,000 years from the Vostok ice core, Antarctica, *Nature*, *399*, 429-436, 1999.

Pichon, J.J., L.D. Labeyrie, G. Bareille, M. Labracherie, M. Duprat, and J. Jouzel, Surface waters temperature changes in the high latitudes of the southern ocean over the last glacial-interglacial cycle, *Paleoceanography*, *7*, 289-318, 1992.

Raisbeck, G.M., F. Yiou, D. Bourles, C. Lorius, J. Jouzel, and N.I. Barkov, Evidence for two intervals of enhanced deposition in Antarctic ice during the last glacial period, *Nature*, *326*, 273-277, 1987.

Raisbeck, G.M., F. Yiou, E. Bard, D. Dollfus, J. Jouzel, and J.R. Petit, Absolute dating of the last 7000 years of the Vostok ice core using ^{10}Be, *Mineralogical Magazine*, *62A*, 1228, 1998.

Raymo, M.E., and M. Horowitz, Organic carbon paleo-pCO_2 and marine-ice core correlations and chronology, *Geophys. Res. Lett.*, *23*(4), 367-370, 1996.

Ritz, C., Un modèle thermo-mécanique d'évolution pour le bassin glaciaire Antarctique Vostok-Glacier Byrd: Sensibilité aux valeurs des paramètres mal connus, Univ. J. Fourier, Grenoble, France, 1992.

Salamatin, A.N., V.Y. Lipenkov, N.I. Barkov, J. Jouzel, J.R. Petit, and D. Raynaud, Ice core age dating and paleothermometer calibration on the basis of isotopes and temperature profiles from deep boreholes at Vostok Station (East Antarctica), *J. Geophys. Res.*, *103*, 8963-8977, 1998a.

Salamatin, A.N., R.N. Vostretov, J.R. Petit, V.Y. Lipenkov, and N.I. Barkov, Geophysical and paleoclimatic implications of the stacked temperature profile from the deep borehole at Vostok station (Antarctica), *Mat. Glyatsiol.*, *85*, 233-240, 1998b.

Schramm, A., M. Stein, and S.L. Goldstein, Calibration of the ^{14}C time scale to >40 kyr by ^{234}U-^{230}Th dating of the Lake Lisan sediments (last glacial Dead Sea), *Earth Planet. Sci. Lett.*, *175*, 27-40, 2000.

Schwander, J., T. Sowers, J.-M. Barnola, T. Blunier, A. Fuchs, and B. Malaizé, Age scale of the air in the summit ice: implication for the glacial-interglacial temperature change, *J. Geophys. Res.*, *102*, 19,483-19,493, 1997.

Schwander, J., J. Jouzel, C.U. Hammer, J.-R. Petit, R. Udisti, and E. Wolff, A tentative chronology of the EPICA Dome C ice core, *Geophys. Res. Lett.*, in press, 2001.

Shackleton, N.J., The 100,000-year Ice-age cycle identified and found to lag temperature, CO_2 and orbital eccentricity, *Science*, 1897-1902, 2000.

Shackleton, N.J., J. Le, A. Mix, and M. Hall, Carbon isotope records from Pacific surface waters and atmospheric carbon dioxide, *Quat. Sci. Rev.*, *11*, 387-400, 1992.

Sowers, T., M. Bender, L.D. Labeyrie, J. Jouzel, D. Raynaud, D. Martinson, and Y.S. Korotkevich, 135 000 year Vostok - SPECMAP common temporal framework, *Paleoceanography*, *8* (6), 737-766, 1993.

Tarantola, A., *Inverse Poblem Theory: Methods for Data Fitting and Model Parameter Estimation*, Elsevier Sci., New York, 1987.

Vimeux, F., V. Masson, J. Jouzel, M. Stievenard, and J.R. Petit, Glacial-Interglacial changes in ocean surface conditions in the Southern Hemisphere, *Nature*, *398*, 410-413, 1999.

Vimeux, F., V. Masson, G. Delaygue, J. Jouzel, J.R. Petit, and M. Stievenard, A 420,000 year deuterium excess record from East Antarctica: information on past changes in the origin of precipitation at Vostok, *J. Geophys. Res.*, this issue.

Waelbroeck, C., J. Jouzel, L. Labeyrie, C. Lorius, M. Labracherie, and M. Stievenard, A comparison of the Vostok ice deuterium record and series from Southern Ocean core MD 88-770 over the last two glacial-interglacial cycles, *Clim. Dyn.*, *12*, 113-123, 1995.

Werner, M., M. Heimann, and G. Hoffmann, Isotopic composition and origin of the polar precipitation in present and glacial climate simulations, *Tellus*, 603-612, 2000.

Yiou, F., et al., Beryllium 10 in the Greenland Ice Core Project ice core at Summit Greenland, *J. Geophys. Res.*, *102*, 26,783-26,794, 1997.

J. Jouzel, and C. Waelbroeck, Laboratoire des Sciences du Climat et de l'Environnement, IPSL, UMR CEA/CNRS No. 1572, Orme des Merisiers, CEA Saclay, 91191 Gif-sur-Yvette, France. (jouzel@lsce.saclay.cea.fr, waelbroeck@lsce.saclay.cea.fr)

J.-M. Barnola, F. Parrenin, and C. Ritz, Laboratoire de Glaciologie et Géophysique de l'Environnement, CNRS, B.P 96 Domaine Universitaire, 38402 Saint-Martin-d'Hères Cedex, France. (barnola@glaciog.ujf-grenoble.fr, parrenin@glaciog.ujf-grenoble.fr, catritz@glaciog.ujf-grenoble.fr)

(Received July 17, 2000; revised March 26, 2001; accepted March 30, 2001.)